Crystallographic analysis of *Staphylococcus aureus* LcpA, the primary wall teichoic acid ligase

Franco K. K. Li[1,2], Federico I. Rosell[1,2], Robert T. Gale[3], Jean-Pierre Simorre[4], Eric D. Brown[3], Natalie C. J. Strynadka[1,2*]

From the [1]Department of Biochemistry and Molecular Biology, The University of British Columbia, Vancouver, British Columbia, Canada; [2]Centre for Blood Research, The University of British Columbia, Vancouver, British Columbia, Canada; [3]Department of Biochemistry and Biomedical Sciences, Michael G. DeGroote Institute for Infectious Disease Research, McMaster University, Hamilton, Ontario, Canada; [4]Univ. Grenoble Alpes, CNRS, CEA, Institut de Biologie Structurale (IBS), 71 avenue des Martyrs, 38000, Grenoble, France.

Running Title: Crystallographic analysis of LytR-CpsA-Psr enzymes

*To whom correspondence should be addressed: Natalie C.J. Strynadka: Department of Biochemistry and Molecular Biology, The University of British Columbia, Life Sciences Centre, 2350 Health Sciences Mall, Vancouver, BC V6T 1Z3, Canada; ncjs@mail.ubc.ca; Tel. (604) 822-7729; Fax. (604) 822-5227.

TABLE OF CONTENTS

Table S1. List of LCP enzyme structures

PDB ID	Enzyme	Resolution (Å)	Ligands at substrate binding sites	Sequence identity compared to *S. aureus* LcpA (%)		Cα RMSD compared to *S. aureus* LcpA		Year	Publication
				Overall	Structure	Structure	Active site[a]		
6UEX	*S. aureus* LcpA	1.90	C_{40}-PP-GlcNAc	100	100	-	-	2019	This work
6UF5	*B. subtilis* TagT	2.80	-	25.9	31.5	3.40 Å over 214 residues	0.85 Å over 10 residues		
6UF6	*B. subtilis* TagU (SeMet)	2.20	-	26.2	28.8	5.60 Å over 222 residues	2.02 Å over 10 residues		
6UF3	*B. subtilis* TagV	1.60	-	27.4	28.8	3.19 Å over 235 residues	1.10 Å over 10 residues		
5V8C	*Actinomyces oris* LytR-Csp2A-Psr	2.51	PEG4000 and PO_4^{3-}	18.3	19.2	6.01 Å over 216 residues	2.00 Å over 10 residues	2019	Doi: 10.1128/mBio.01580-18 (1)
6MPT	*B. subtilis* TagT	1.65	C_{30}-PP-GlcNAc	25.9	29.1	3.35 Å over 215 residues	1.04 Å over 10 residues	2018	Doi: 10.1021/jacs.7b13551 (2)
6MPS	*B. subtilis* TagT	1.86	C_{30}-PP-GlcNAc-ManNAc and Mg^{2+}	25.9	29.1	3.22 Å over 216 residues	0.85 Å over 10 residues		
4OBM	*Eubacterium siraeum* DSM 15702 EUBSIR_01389	2.15	Tetraethylene glycol and PEG 400	14.7	15.8	5.94 Å over 227 residues	2.54 Å over 10 residues	2014	Joint Center for Structural Genomics (JCSG)
4DE9	*B. subtilis* TagT	1.79	C_{40}-PP	25.9	29.1	3.06 Å over 208 residues	0.97 Å over 9 residues	2012	Doi: 10.1089/mdr.2011.0232 (3)
4DE8	*S. pneumoniae* Cps2A (R267A)	1.95	C_{40}-P	23.8	22.5	5.66 Å over 241 residues	1.07 Å over 10 residues		
2XXP	*S. pneumoniae* Cps2A	1.69	C_{50}-P (mono-trans, octa-cis)	23.8	22.9	5.62 Å over 241 residues	1.02 Å over 10 residues	2011	Doi: 10.1038/emboj.2011.358 (4)
3TEP	*S. pneumoniae* Cps2A	2.03	C_{40}-PP and Mg^{2+}	23.8	22.9	5.73 Å over 241 residues	0.95 Å over 10 residues		
3TFL	*S. pneumoniae* Cps2A	2.05	C_{40}-PP	23.8	22.9	5.55 Å over 240 residues	1.02 Å over 10 residues		
2XXQ	*S. pneumoniae* Cps2A (R267A)	1.77	C_{40}-PP	23.8	22.5	5.64 Å over 241 residues	1.01 Å over 10 residues		
3TEL	*S. pneumoniae* Cps2A	1.80	C_{40}-PP and Mn^{2+}	23.8	22.5	5.62 Å over 241 residues	1.05 Å over 10 residues		
3QFI	*Enterococcus faecalis* EF0465	2.71	-	26.1	28.4	2.53 Å over 227 residues	1.09 Å over 9 residues	2011	Northeast Structural Genomics Consortium (NESG)
3NXH	*B. subtilis* TagV	2.59	-	27.4	32.5	3.98 Å over 201 residues	1.61 Å over 8 residues	2010	
3PE5	*Clostridium leptum* A7VV38_9CLOT	2.38	-	26.4	27.9	3.64 Å over 241 residues	3.66 Å over 10 residues (chain B)	2010	
3OWQ	*Listeria innocua* Lin1025	2.61	Di(hydroxyethyl)ether	22.0	24.9	4.39 Å over 228 residues	2.85 Å over 10 residues (chain A)	2010	
3NRO	*Listeria monocytogenes* Lmo1026	2.90	-	22.4	25.3	4.57 Å over 219 residues	2.93 Å over 10 residues (chain B)	2010	
3MEJ	*B. subtilis* TagT	2.49	-	25.9	29.1	3.08 Å over 218 residues	1.46 Å over 10 residues	2010	
3OKZ	*Streptococcus algalactiae* gbs0355	2.70	-	25.7	25.9	3.42 Å over 235 residues	0.89 Å over 10 residues (chain A)	2010	

[a] Active site RMSD values were calculated with 10 conserved active site residues (*S. aureus* LcpA D91, R99, D101, R122, D123, K135, R216, R218, D224, R227).

Table S2. Summary of mutagenesis analyses of LCP enzymes

$LcpA_{SA}$ residue	Location/proposed role	Mutagenesis analysis
D91	Mg^{2+} coordination	• $LcpB_{SA}$ (31-405) D70A – No activity *in vitro* (2) • $TagT_{BS}$ (46-323) D82A – Significant decrease in activity *in vitro* (2) • $TagU_{BS}$ D75A – Unable to sustain growth in the absence of WT TagT, TagU and TagV (4) • $LcpA_{CG}$ D88A – Failed to complement growth when WT LcpA expression was suppressed. Recombinant enzyme has pyrophosphatase activity *in vitro* (5)
R99	PG binding	• $TagU_{BS}$ R83A – Unable to sustain growth in the absence of WT TagT, TagU and TagV (4) • $LcpA_{AO}$ R128A – Glycosylation of GspA was unaffected (1)
D101	Mg^{2+} coordination	• $TagT_{BS}$ (46-323) D97A – No activity *in vitro* (2) • $TagU_{BS}$ D85A – Unable to sustain growth in the absence of WT TagT, TagU and TagV (4)
S102	Interior of lipid binding pocket	• $TagU_{BS}$ T86F – Unable to sustain growth in the absence of WT TagT, TagU and TagV (4)
R122	General base	• $TagT_{BS}$ (46-323) R118A – No activity *in vitro* (2) • $LcpA_{CG}$ R138A – Failed to complement growth when WT LcpA expression was suppressed. Recombinant enzyme has pyrophosphatase activity *in vitro* (5) • $LcpA_{AO}$ R149A – Glycosylation of GspA was defective (equivalent to the Δ*lcpA* mutant). Recombinant enzyme has no pyrophosphatase activity *in vitro* (1)
D123	Activation of general base	• $TagT_{BS}$ (46-323) D119T – No activity *in vitro* (2)
K135	PG binding	• $TagT_{BS}$ (46-323) K131A – No activity *in vitro* (2)
E146	Solvent exposed surface of helix 2	• $LcpA_{SA}$ E146K – Increased resistance to vancomycin (6)
A215	Interior of lipid binding pocket	• $TagU_{BS}$ T197F – Unable to sustain growth in the absence of WT TagT, TagU and TagV (4)
R216	General acid	• $LcpA_{CG}$ R257A – Failed to complement growth when WT LcpA expression was suppressed. Recombinant enzyme has pyrophosphatase activity *in vitro* (5)
R218	Donor substrate binding	• $TagT_{BS}$ (46-323) R219A – No activity *in vitro* (2)
D224	PG binding	• $TagT_{BS}$ (46-323) D224A – Significant decrease in activity *in vitro* (2)
R227	Donor substrate binding	• $TagT_{BS}$ (46-323) R227A – No activity *in vitro* (2) • $LcpA_{AO}$ R266A – Glycosylation of GspA was defective (equivalent to the Δ*lcpA* mutant) (1)
($LcpA_{AO}$ C179)	Helix 2; stability of actinobacterial LCP proteins	• $LcpA_{AO}$ C179A/C365A – Glycosylation of GspA was reduced. Recombinant enzyme displays low thermostability and reduced pyrophosphatase activity *in vitro* (1)
($LcpA_{AO}$ C365)	C-terminus; stability of actinobacterial LCP proteins	• $LcpA_{AO}$ C365A – Glycosylation of GspA was reduced (1) • $LcpA_{AO}$ C179A/C365A – Glycosylation of GspA was reduced. Recombinant enzyme displays low thermostability and reduced pyrophosphatase activity *in vitro* (1)

Table S3. Statistics of the top 3 triGlcNAc-bound $LcpA_{SA}$ clusters generated with HADDOCK2.2

Cluster number	1	3	5
HADDOCK score	-47.6 +/- 4.3	-43.0 +/- 1.6	-37.4 +/- 6.4
Cluster size	25	10	8
RMSD from the overall lowest-energy structure (Å)	1.4 +/- 0.8	1.9 +/- 0.1	1.7 +/- 0.1
Van der Waals energy (kcal/mol)	-21.0 +/- 4.2	-24.2 +/- 3.6	-16.7 +/- 3.7
Electrostatic energy (kcal/mol)	-21.6 +/- 18.1	-9.9 +/- 15.7	-29.8 +/- 4.6
Desolvation energy (kcal/mol)	-22.4 +/- 7.0	-17.0 +/- 3.6	-14.8 +/- 6.8
Restraints violation energy (kcal/mol)	1.6 +/- 0.76	2.2 +/- 1.36	1.2 +/- 1.03
Buried Surface Area ($Å^2$)	657.6 +/- 69.2	630.7 +/- 29.0	564.8 +/- 45.5
Z-Score	-2.1	-1.1	0.2

Table S4. Statistics of the top 3 triGlcNAc-bound $TagT_{BS}$ clusters generated with HADDOCK2.2

Cluster number	1	2	3
HADDOCK score	-48.5 +/- 3.0	-45.5 +/- 1.9	-43.6 +/- 2.8
Cluster size	25	16	9
RMSD from the overall lowest-energy structure (Å)	3.6 +/- 0.2	3.8 +/- 0.9	3.1 +/- 0.6
Van der Waals energy (kcal/mol)	-23.4 +/- 1.5	-23.2 +/- 2.1	-22.3 +/- 2.4
Electrostatic energy (kcal/mol)	-51.2 +/- 19.0	-38.9 +/- 16.9	-28.2 +/- 7.3
Desolvation energy (kcal/mol)	-15.0 +/- 7.1	-14.8 +/- 2.8	-16.0 +/- 2.4
Restraints violation energy (kcal/mol)	1.7 +/- 0.33	2.5 +/- 0.95	2.9 +/- 1.05
Buried Surface Area ($Å^2$)	689.9 +/- 27.3	669.9 +/- 46.9	660.7 +/- 44.8
Z-Score	-2.5	-1.2	-0.4

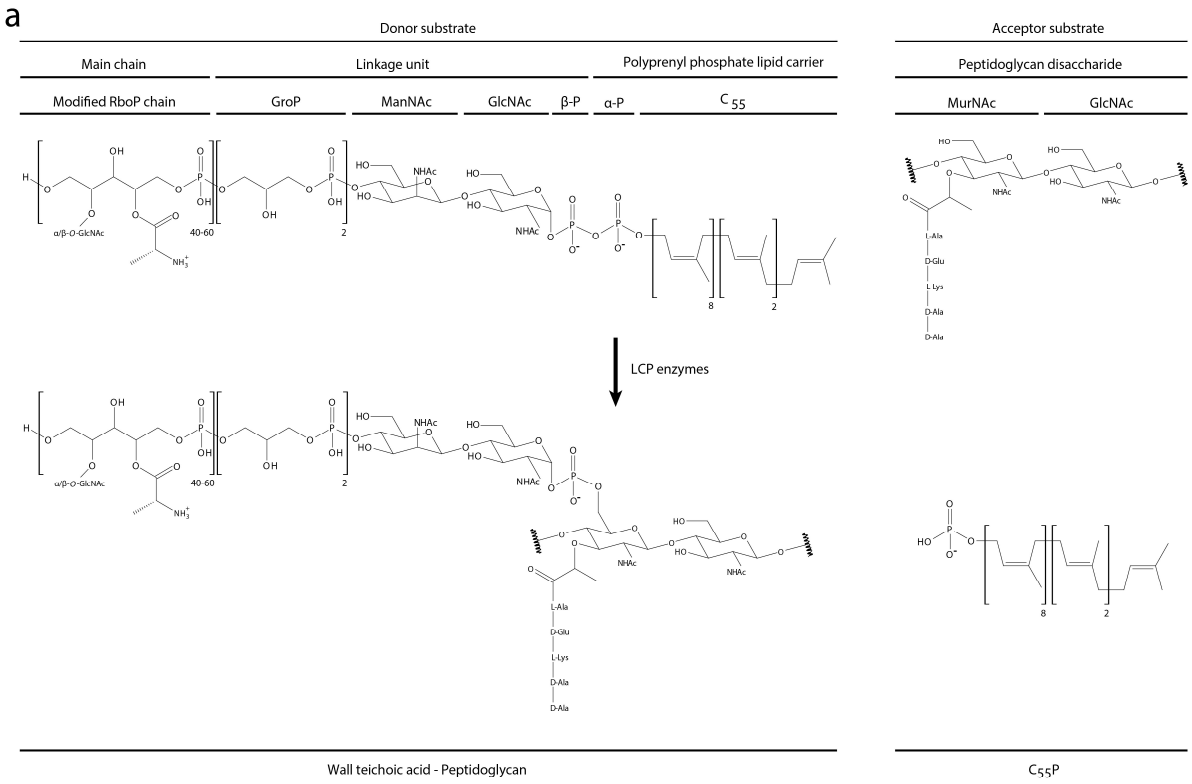

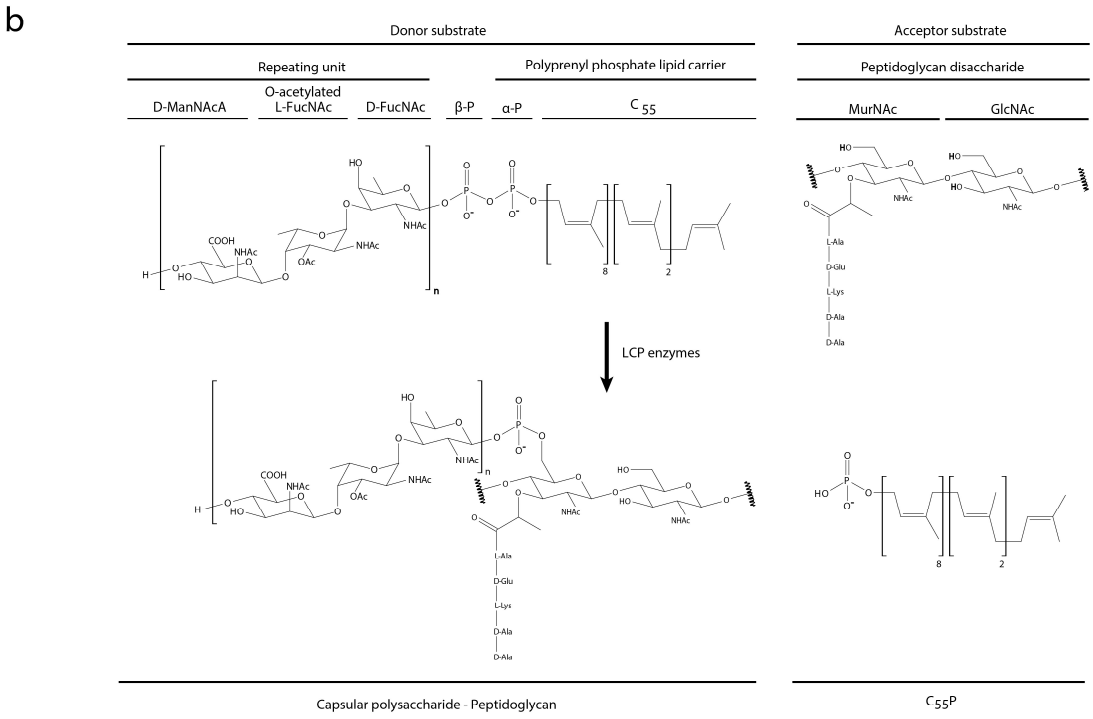

Figure S1. Chemical structures of *S. aureus* LCP enzyme substrates and products. LCP enzymes catalyze the transfer of WTA **(a)** and other anionic polymers, such as capsular polysaccharide **(b),** from lipid carriers (commonly C_{55}-P) to the C6-hydroxyl group of PG MurNAc.

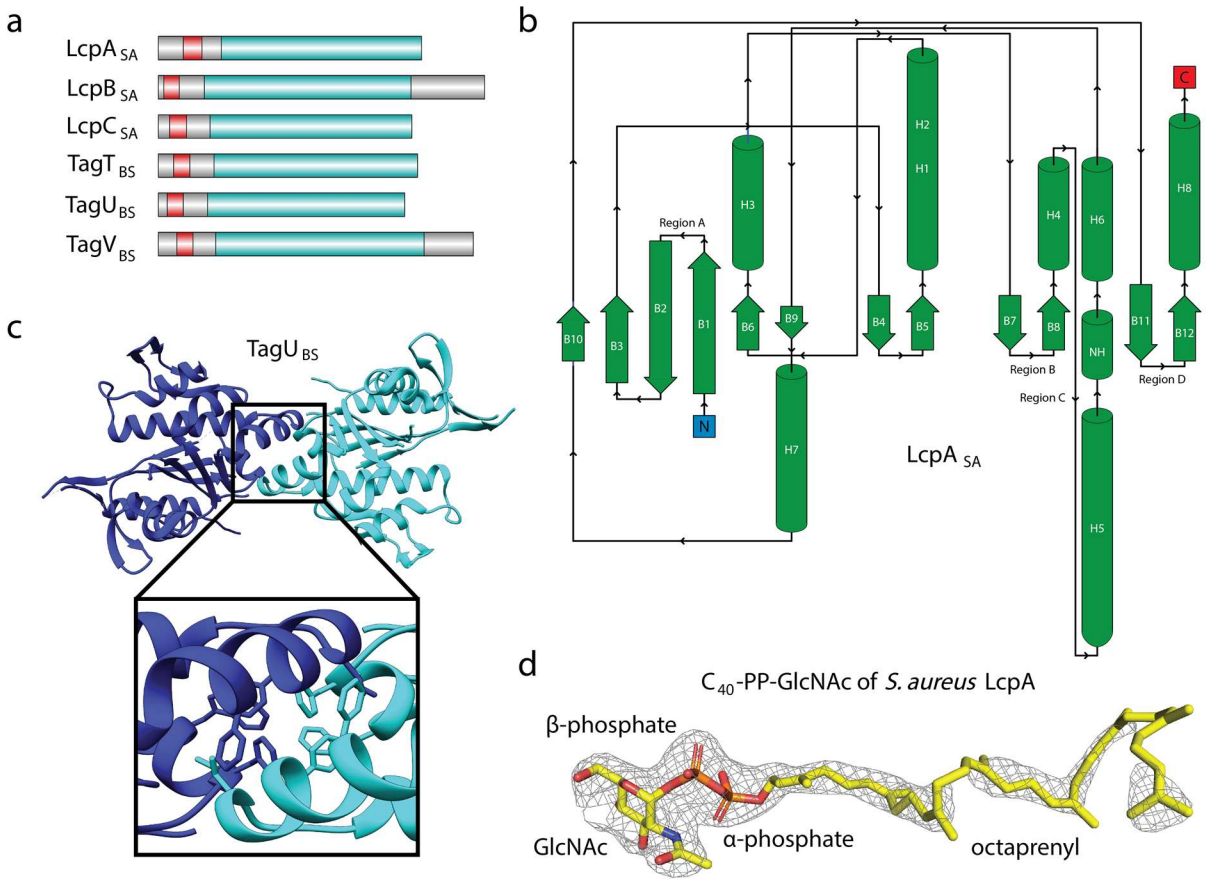

Figure S2. **Domain organization and secondary structure of LCP enzymes. (a)** Domain organization of *S. aureus* (strain N315) and *B. subtilis* (strain 168) LCP enzymes. Transmembrane helices and LCP domains are shown in red and cyan, respectively. **(b)** Secondary structure diagram of $LcpA_{SA}$ (H, helix; B, β-strand; NH, non-conserved helix). **(c)** Crystal packing of two $TagU_{BS}$ monomers. Select residues mediating hydrophobic interactions are depicted as sticks. **(d)** The lipid bound to $LcpA_{SA}$ is shown in yellow with the 2Fo-Fc electron density map contoured to 1σ in a gray mesh. Heteroatoms are coloured by type (O, red; P, orange; N, blue).

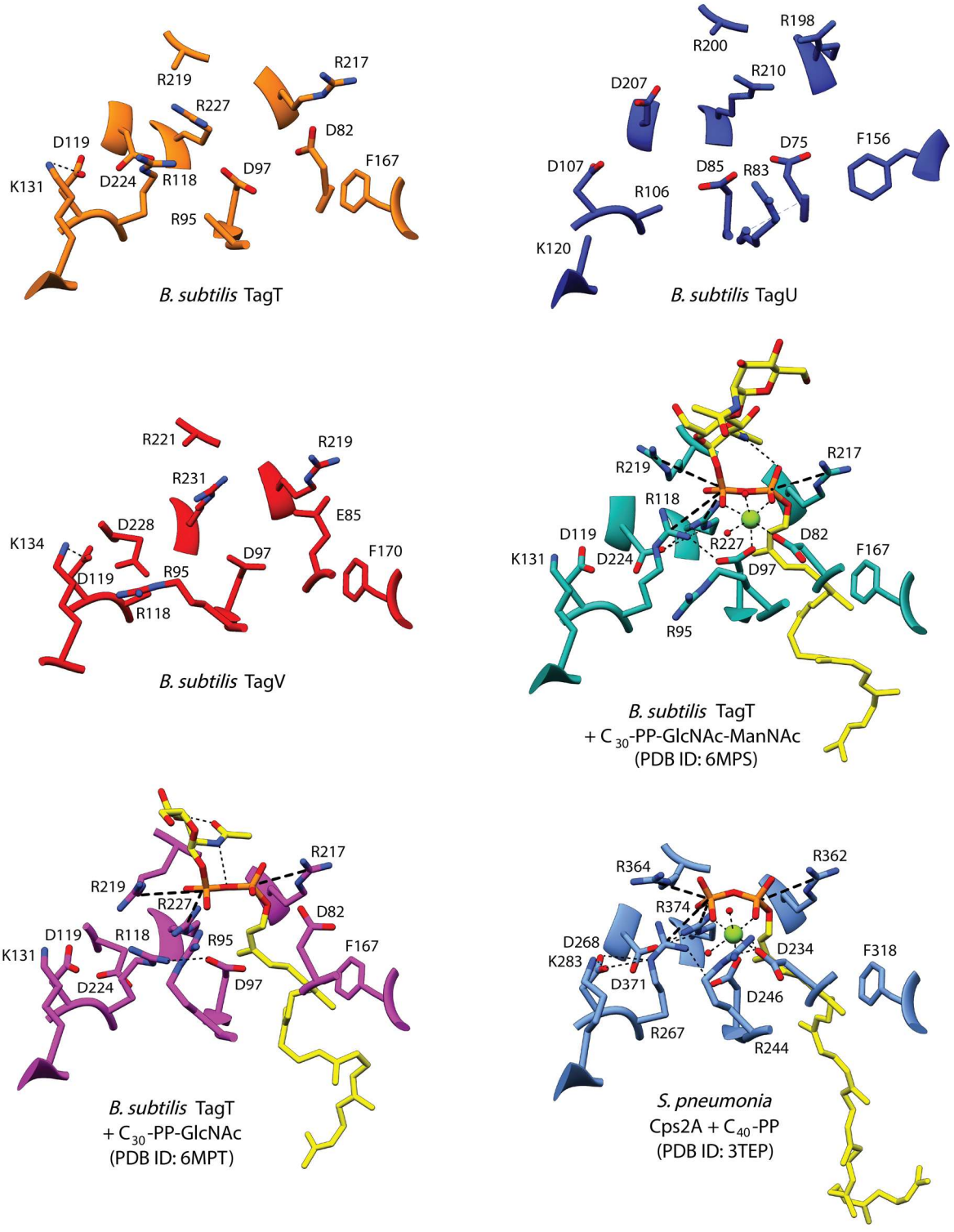

Figure S3. Pyrophosphate-binding site of LCP enzymes. Conserved residues surrounding the pyrophosphate moiety of the lipid substrate (yellow) depicted as sticks. Heteroatoms are coloured by type (O, red; P, orange; N, blue; Mg^{2+}, green) and bonds are indicated by lines (salt bridges as thick dotted lines; hydrogen bonds and metal-coordinating bonds as thin dotted lines).

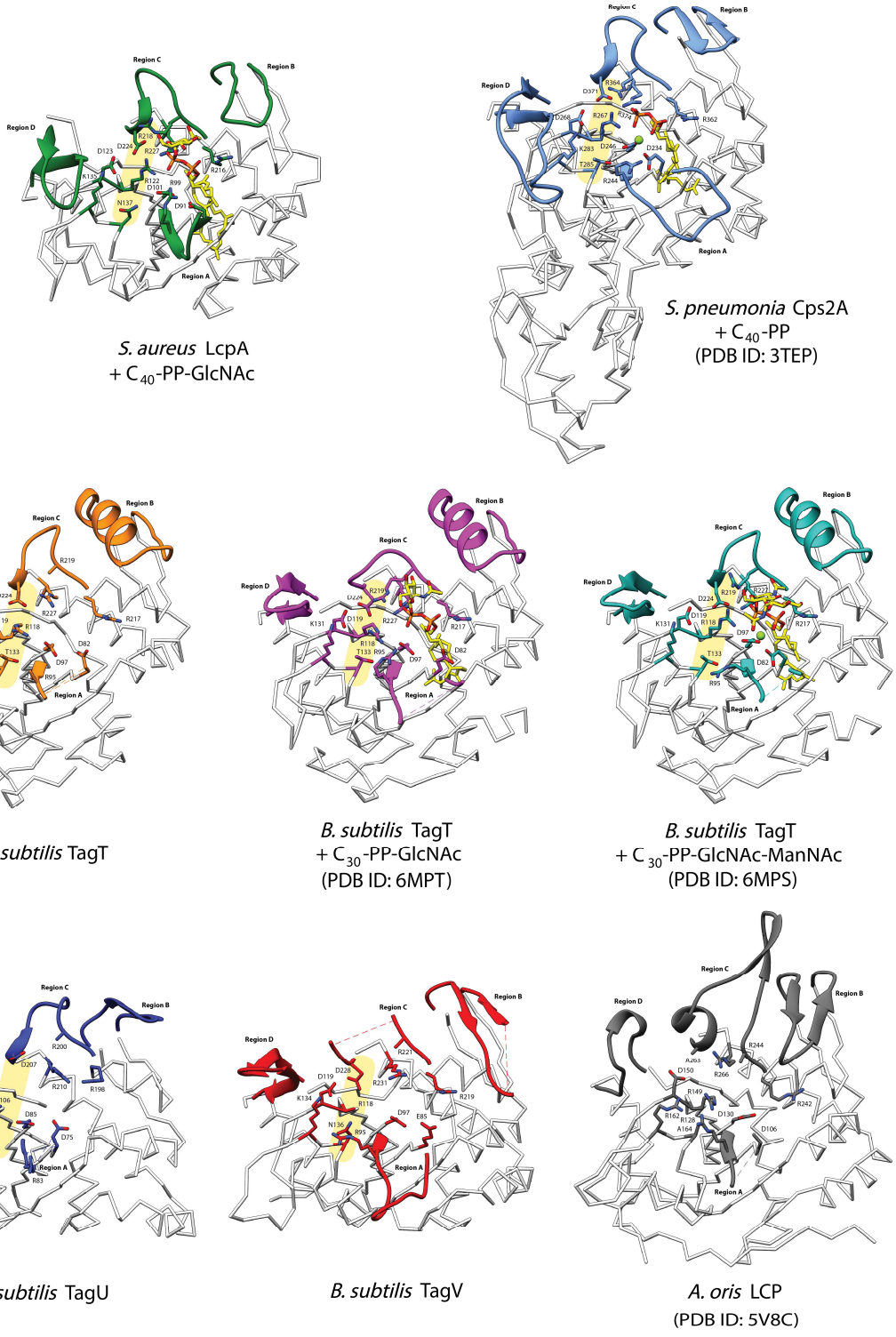

Figure S4. Structural features surrounding the entrance of the lipid-binding pocket. Regions A, B, C and D are shown as coloured ribbons, and lipids are depicted in yellow. Select residues are shown as sticks and heteroatoms are coloured by type (O, red; P, orange; N, blue; Mg^{2+}, green). The putative PG binding site is highlighted in yellow.

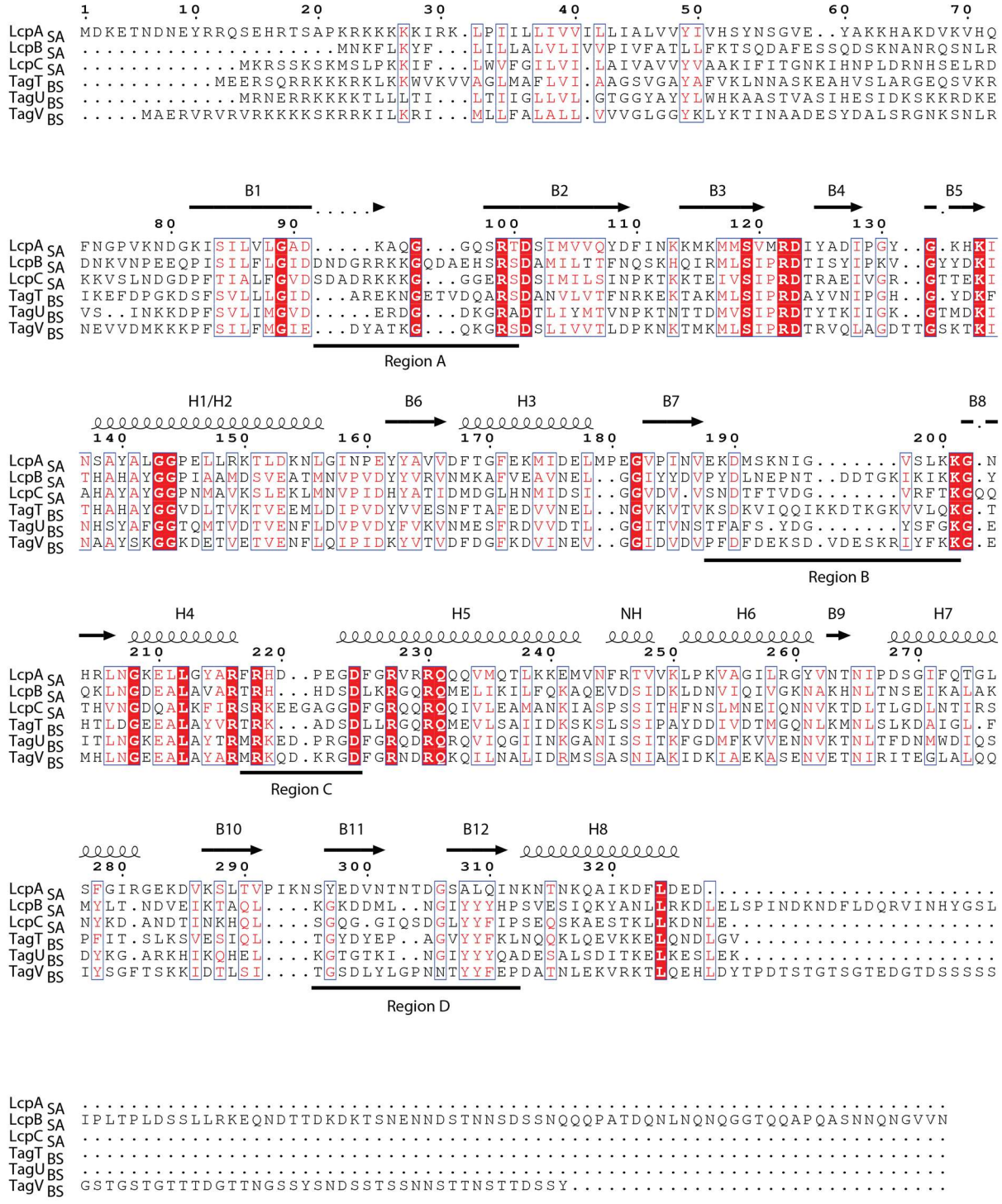

Figure S5. Sequence alignment of *S. aureus* and *B. subtilis* LCP enzymes. Secondary structure of $LcpA_{SA}$ is depicted.

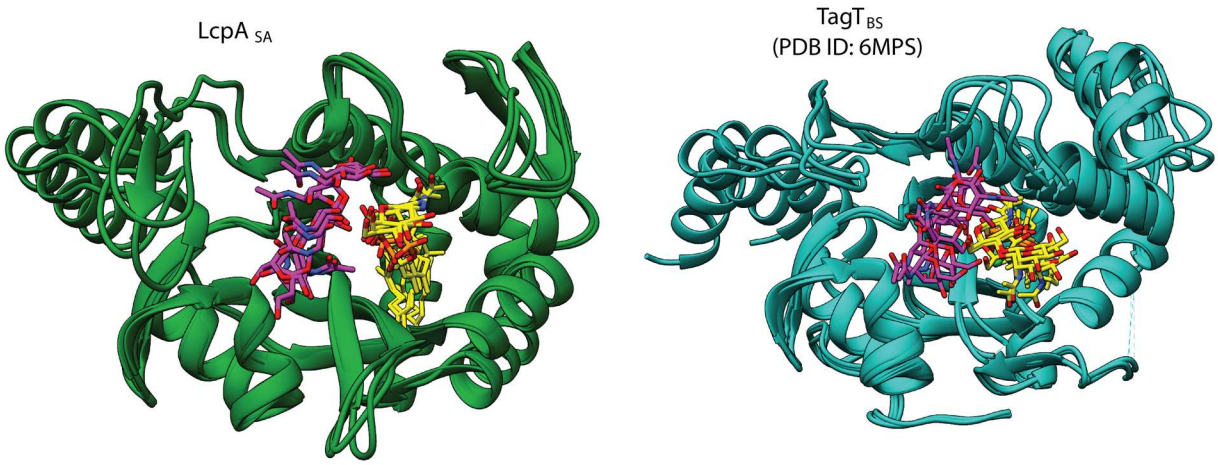

Figure S6. TriGlcNAc docked onto $LcpA_{SA}$ and $TagT_{BS}$. Ribbon structures of $LcpA_{SA}$ (green) and $TagT_{BS}$ (PDB ID: 6MPS; cyan) in the top 3 clusters are depicted complexed to triGlcNAc (purple). The highest scoring structure in each cluster is shown. The lipid is in yellow and heteroatoms are coloured by type (O, red; P, orange; N, blue).

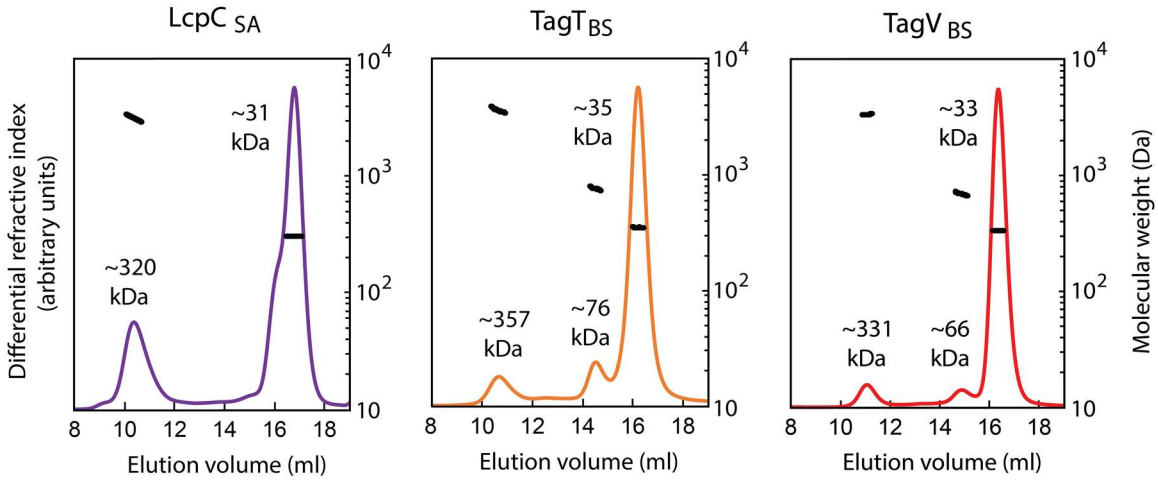

Figure S7. Oligomerization of *S. aureus* and *B. subtilis* LCP enzymes. Representative SEC-MALS analyses of ΔTM LCP enzymes eluted from a Superdex200 10/300 GL column. The coloured lines represent the differential refractive index, and the black lines correspond to the molecular weight. The average molecular weight from 3 trials is reported.

References

1. Siegel, S. D., Amer, B. R., Wu, C., Sawaya, M. R., Gosschalk, J. E., Clubb, R. T., and Ton-That, H. (2019) Structure and Mechanism of LcpA, a Phosphotransferase That Mediates Glycosylation of a Gram-Positive Bacterial Cell Wall-Anchored Protein. *MBio*. **10**, 1–16

2. Schaefer, K., Owens, T. W., Kahne, D., and Walker, S. (2018) Substrate Preferences Establish the Order of Cell Wall Assembly in Staphylococcus aureus. *J. Am. Chem. Soc.* **140**, 2442–2445

3. Eberhardt, A., Hoyland, C. N., Vollmer, D., Bisle, S., Cleverley, R. M., Johnsborg, O., Håvarstein, L. S., Lewis, R. J., and Vollmer, W. (2012) Attachment of capsular polysaccharide to the cell wall in Streptococcus pneumoniae. *Microb. Drug Resist.* **18**, 240–55

4. Kawai, Y., Marles-Wright, J., Cleverley, R. M., Emmins, R., Ishikawa, S., Kuwano, M., Heinz, N., Bui, N. K., Hoyland, C. N., Ogasawara, N., Lewis, R. J., Vollmer, W., Daniel, R. a, and Errington, J. (2011) A widespread family of bacterial cell wall assembly proteins. *EMBO J.* **30**, 4931–41

5. Baumgart, M., Schubert, K., Bramkamp, M., and Frunzke, J. (2016) Impact of LytR-CpsA-Psr Proteins on Cell Wall Biosynthesis in Corynebacterium glutamicum. *J. Bacteriol.* **198**, 3045–3059

6. Katayama, Y., Sekine, M., Hishinuma, T., Aiba, Y., and Hiramatsu, K. (2016) Complete Reconstitution of the Vancomycin-Intermediate Staphylococcus aureus Phenotype of Strain Mu50 in Vancomycin-Susceptible S. aureus. *Antimicrob. Agents Chemother.* **60**, 3730–42